SAND2021-15314C

Sandia National Laboratories

Exceptional service in the national interest

Numerical and Experimental Validation of Coupled Poro-elasto-plasticity of Geomaterials

Maria Warren, Mario J. Martinez,

Alec Kucala, James E. Bean, Hongkyu Yoon

Sandia National Laboratories

Albuquerque, NM, USA

AGU 2021 Fall Meeting

This work was supported by the Laboratory Directed Research and Development program at Sandia National Laboratories.

Sandia National Laboratories is a multimission laboratory managed and operated by National Technology & Engineering Solutions of Sandia, LLC, a wholly owned subsidiary of Honeywell International Inc., for the U.S. Department of Energy's National Nuclear Security Administration under contract DE-NA0003525.

Outline

- Introduction
- Methodology
  - Coupling methods for poroelasticity
  - Kayenta Plasticity Model
- One-Dimensional Terzaghi Problem
- Two-Dimensional Galin Plate Problem
- Conclusions and Future Work

Introduction

- Sustainable subsurface energy activities, such as carbon sequestration, nuclear waste disposal and geothermal recovery, are coupled poromechanics problems [1]
- Governing equations of poroelasticity: (1) and (2)
- Advantages of Fixed Stress Scheme over Fully Coupled monolithic scheme [2]:
  - Reduce computational demand
  - Unconditional stability
  - Use of multiple modules
- Here, we utilize Sandia **Kayenta** [3] material model within the fixed stress scheme

$$\left(K + \frac{1}{3}G\right)\frac{\partial \epsilon_{kk}}{\partial x_i} + G\nabla^2 u_i = \alpha \frac{\partial \mathrm{p}}{\partial x_i} - b_i \quad (1)$$

$$\alpha \frac{\partial \epsilon_{kk}}{\partial t} + S\frac{\partial p}{\partial t} = \nabla \cdot \left(\frac{k}{\mu}\nabla p\right) \quad (2)$$

K – bulk modulus
G – shear modulus
ϵ_{kk} – volumetric strain
x_i – coordinate reference frame
u – displacement
α – Biot's coefficient
p – pore pressure
b_i – body forces
t – time
S – storativity
k – intrinsic permeability
μ – fluid viscosity

Methodology

- Sandia Sierra Multiphysics toolkit
  - Thermal/Fluid mechanics module: Sierra/Aria [4]
  - Solid mechanics module: Sierra/SM [5]
- Fixed stress scheme: set rate of total mean stress as constant from the solution at the previous iteration
- Implement fixed stress scheme into Sierra
  - Sierra/Aria and Sierra/SM using Sierra/Arpeggio [6]
- Evaluate implementation of plasticity through comparison with 1D analytical solutions [7]
- Then, extend into 2D problem and compare with analytical solution [9]

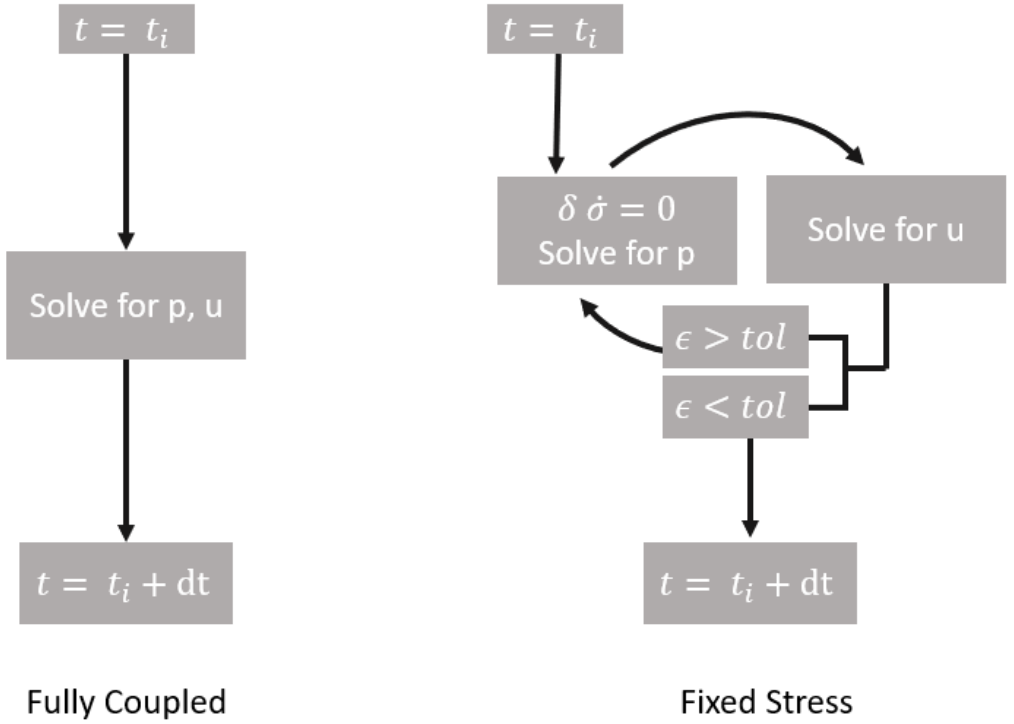

Schematic of coupling schemes over a single time step. The fixed stress scheme iterates based on comparison of error, ϵ, with tol, the global residual tolerance

Kayenta Material Model [3]

- Constitutive model that generates a differentiable yield surface
- Models inelasticity, including phenomena such as microcracking, pore collapse
- Can be used to generate a simpler yield surface, such as von Mises, or calibrated to extensively experimental data
- Failure envelope:

$$F_f = a_1 - a_3 e^{-a_2 I_1} + a_4 I_1$$

Table 1. Mechanical and hydrological properties of geomaterials in simulations[1,2]

	1D Benchmark	2D Benchmark
Material	Saline Aquifer [1]	Sandstone [8]
α	1	-
ϕ_0	0.15	-
v	0.2	0.38
k (m^2)	3.E-14	-
Yield function	Druker-Prager	Tresca
K (GPa)	1.11	1.98
G (GPa)	0.833	0.500
A1	6.12e6	160e6
A4	0.149	-

[1] All geomaterials in this work are modeled with isotropic material properties.
[2] For all materials, reference density of pore fluid is $\rho=1\ g/cm3$

Benchmark Problems for Verification

Evaluate through comparison with analytical solutions:

1. One-Dimensional (1D) Consolidation [7]
   - Plasticity starts at the drainage boundary and proceeds towards the undrained end

2. Two-Dimensional (2D) Galin Plate [9]
   - Plasticity starts at the edges of the central hole and extends into the plate
   - For the loading conditions in these analyses, plastic boundary is an ellipse

1D consolidation

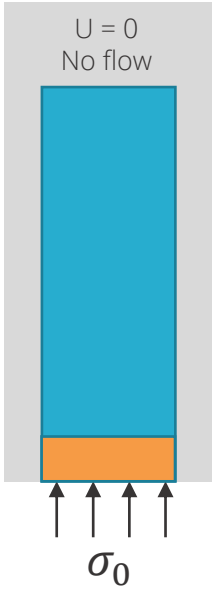

2D Galin Plate

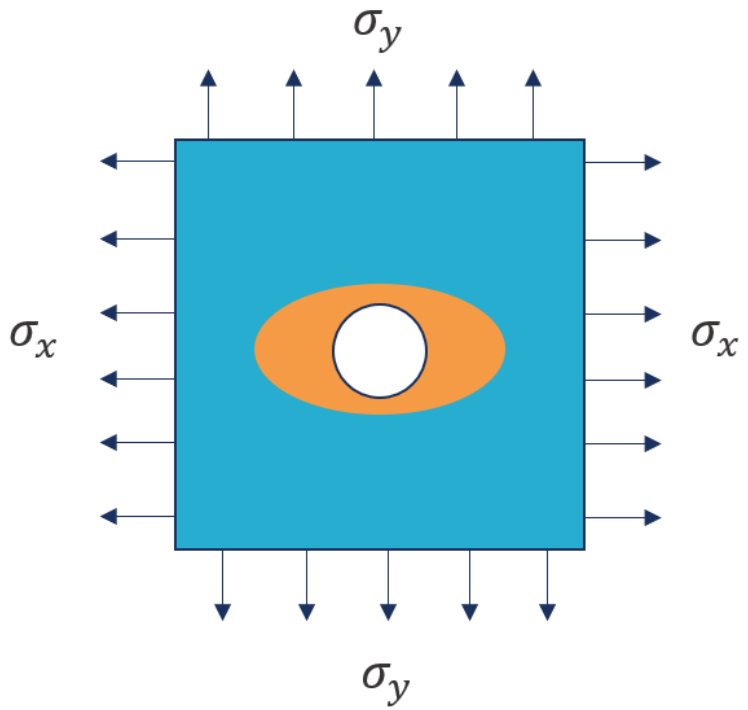

1D Elasto-plastic Consolidation

- Loading conditions
  - Case 1 - Fully Elastic Case
  - Case 2 - Elasto-plastic Case
  - Case 3 - Fully Plastic Case
- Boundary conditions
  - Restrained lateral displacement
  - Along lower boundary, pore fluid drainage and unrestrained z – displacement
- Model details
  - Saline Aquifer material [1]
  - Druker-Prager criteria
  - 50m height of column, with 200 equally-sized elements
- Analytical solution from Liu et al. [6]
- Solution using Sierra/Arpeggio
  - Aria for p
  - Solid Mechanics for u

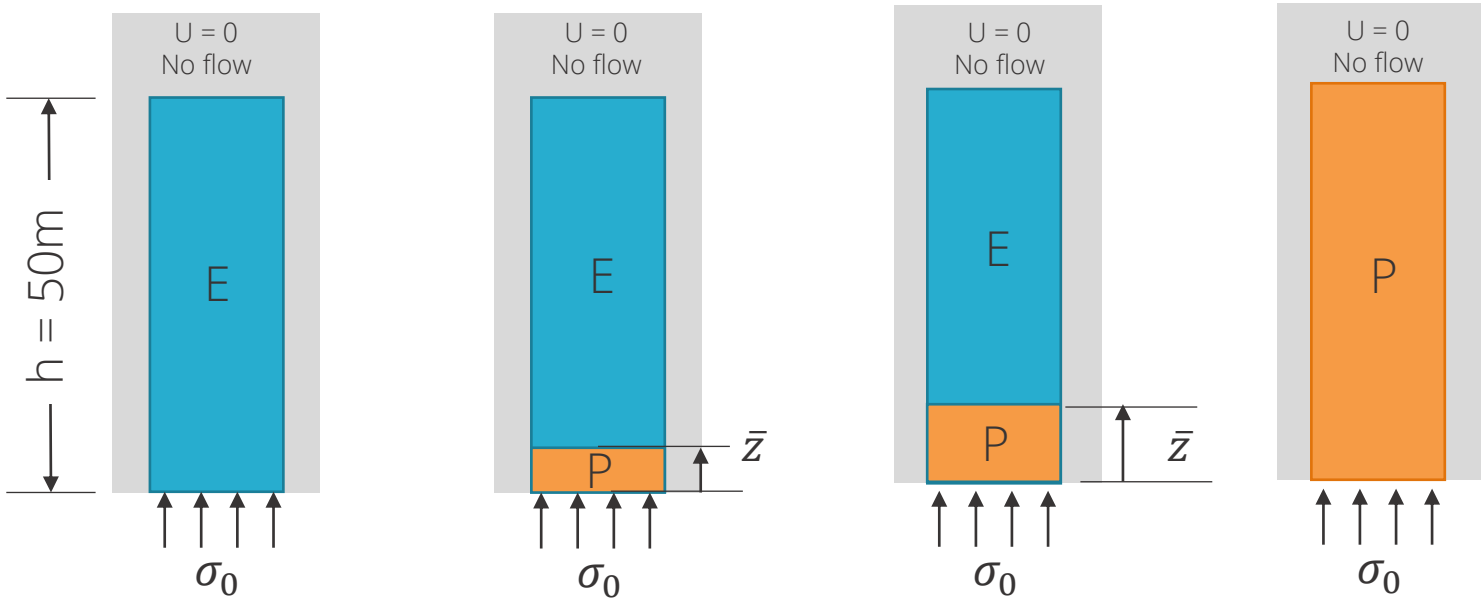

Schematic of 1-D Elastoplastic column, showing the plastic boundary, $\bar{z}$, as it gradually progresses along the column from the drainage boundary

Case 1 – Fully Elastic

$\sigma_0 = 25MPa$

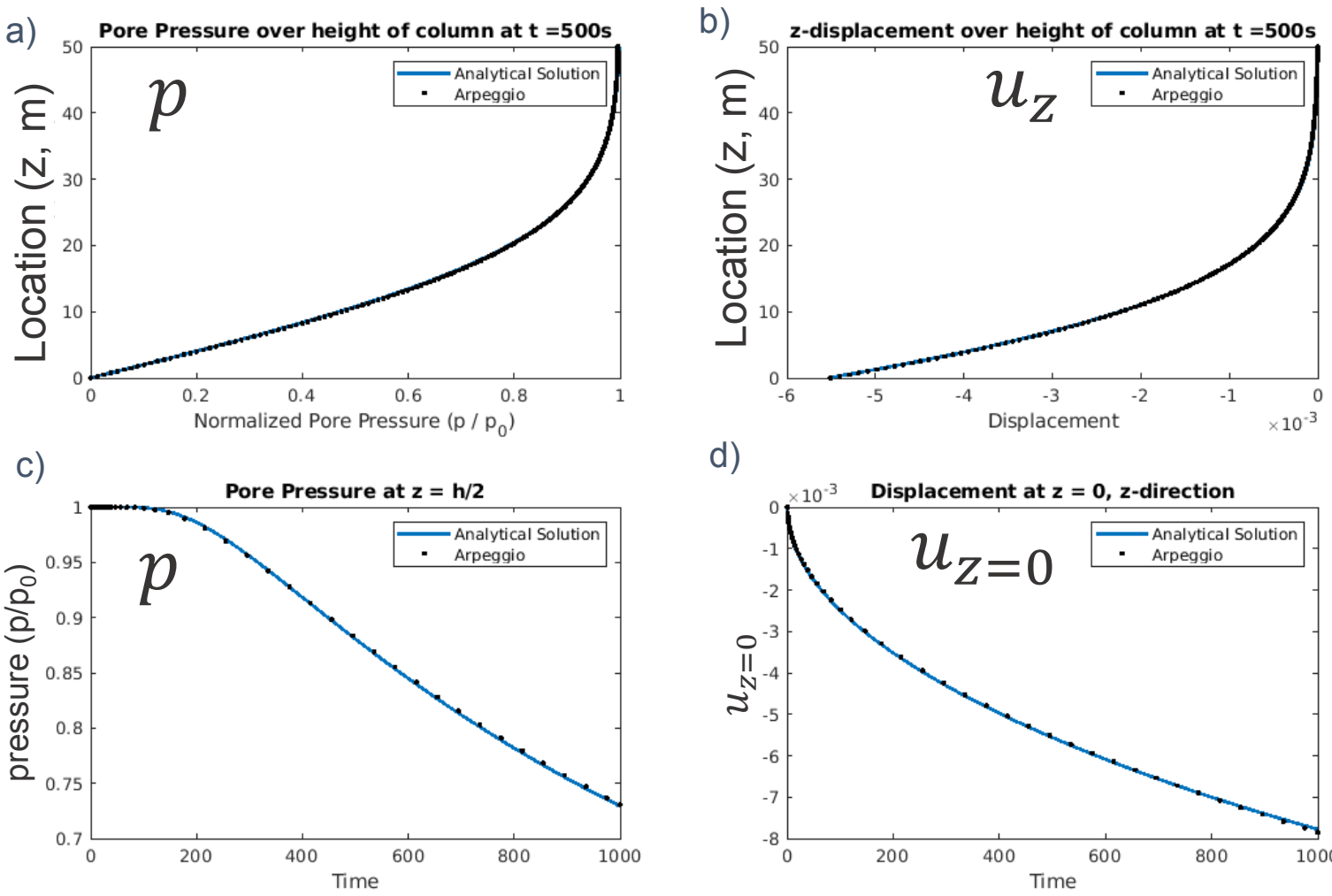

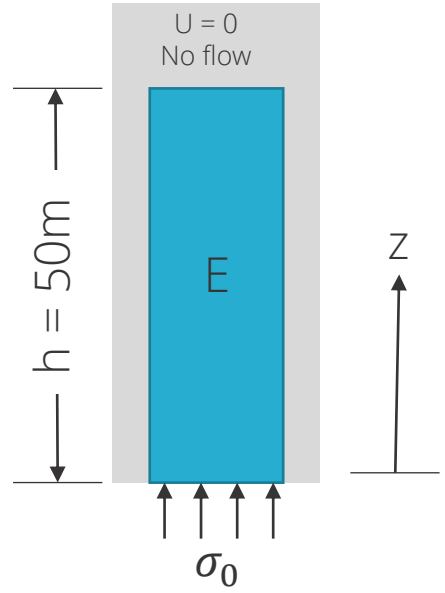

Plots comparing the Sierra/Arpeggio solution to the Analytical solution, for a) Pore pressure along the height of the column, b) Displacement in the z-direction along the height of the column, c) Time history of the pore pressure at mid-height, and d) Time history of displacement at the drainage boundary (z = 0).

Case 2 – Elasto-plastic

$\sigma_0 = 45MPa$

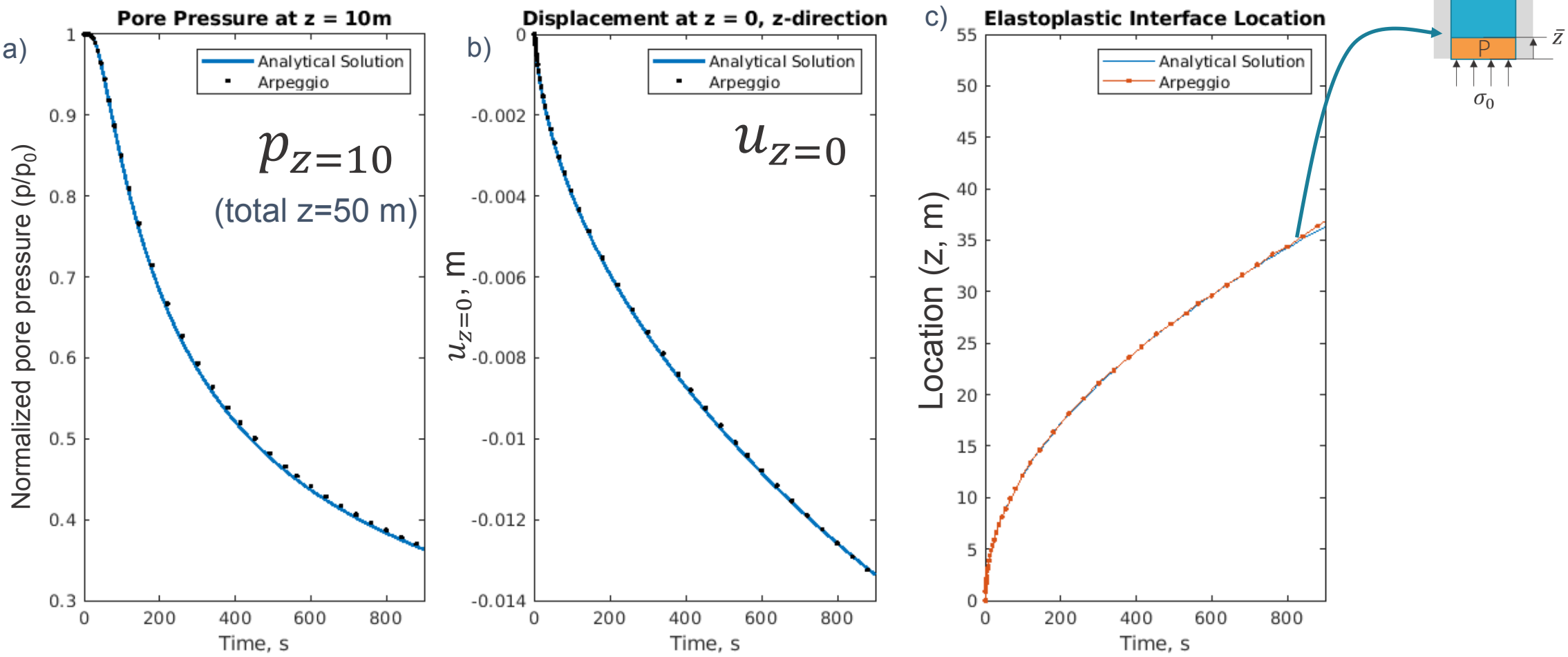

Plots comparing the Sierra/Arpeggio solution to the Analytical solution, a) Time history of the pore pressure at 10m from the drainage boundary, b) Time history of displacement at the drainage boundary (z = 0), and c) Time history of the location of the elasto-plastic interface, showing its progression along the height of the column over time

Case 3 – Fully Plastic

$\sigma_0 = 50MPa$

a)

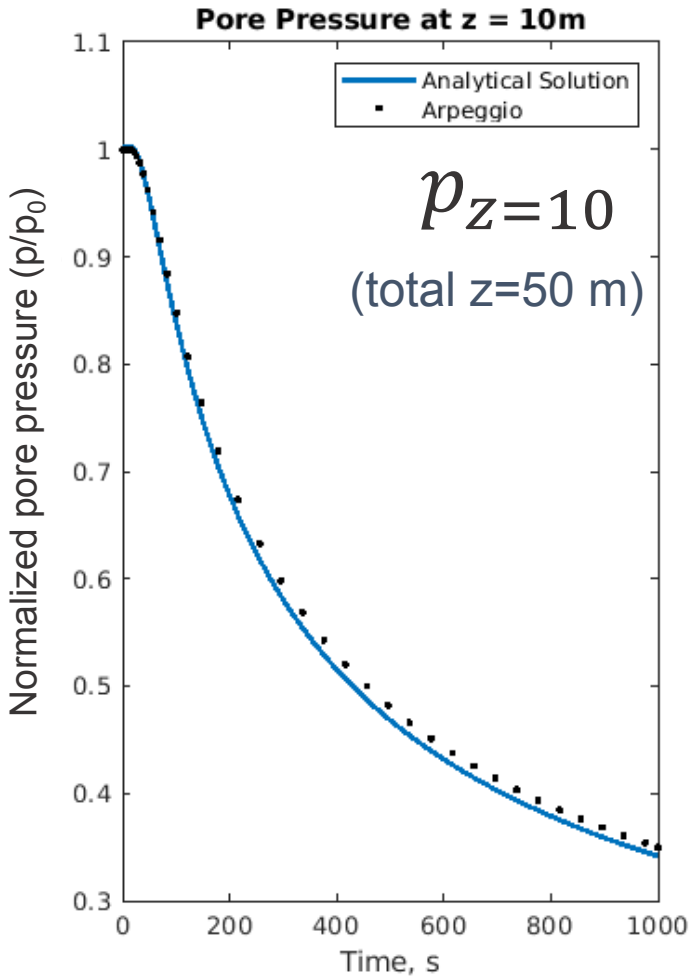

b)

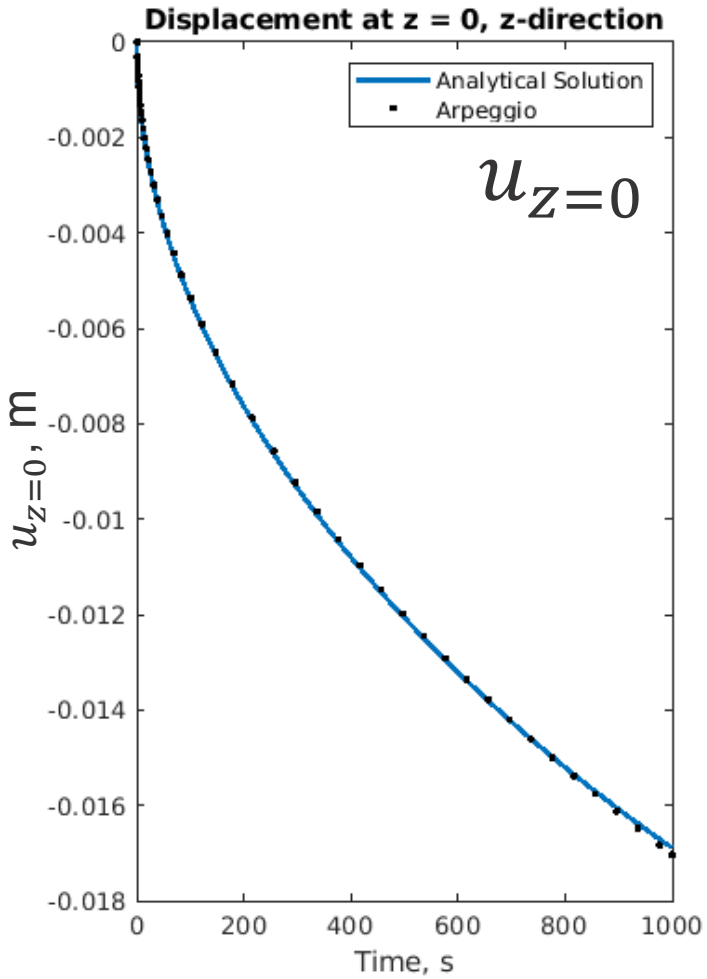

c)

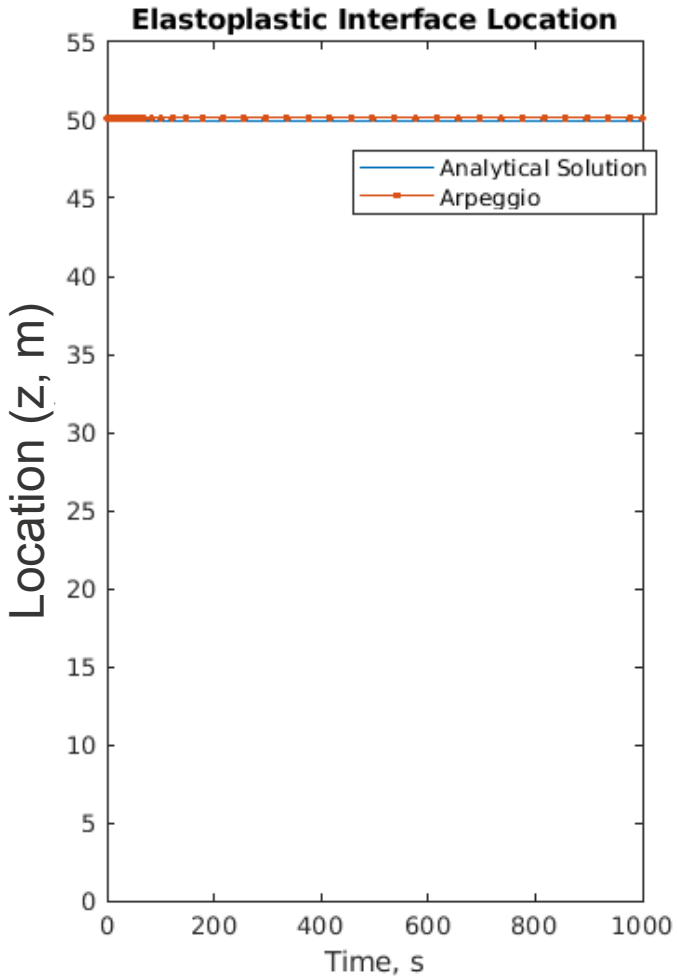

Plots comparing the Sierra/Arpeggio solution to the Analytical solution, a) Time history of the pore pressure at 10m from the drainage boundary, b) Time history of displacement at the drainage boundary (z = 0), and c) Time history of the location of the elasto-plastic interface at h = 50, showing full plasticity along the height of the column

2D Galin Plate

- Problem information
  - $\sigma_x = -247MPa$ (Compression)
  - $\sigma_y = -273MPa$ (Compression)
  - Quarter model of 1m x 1m plate
  - Hole radius = 0.025m
- Boundary conditions
  - Restrained lateral displacement
  - Symmetric boundary conditions to model quarter of plate
  - Plane strain
- Modeling Details
  - Sandstone [8]
  - Tresca Yield Criteria
  - Coarse mesh and fine mesh
- Analytical solution from Yarushina et al. [9]
- Sierra SM (no fluid flow)

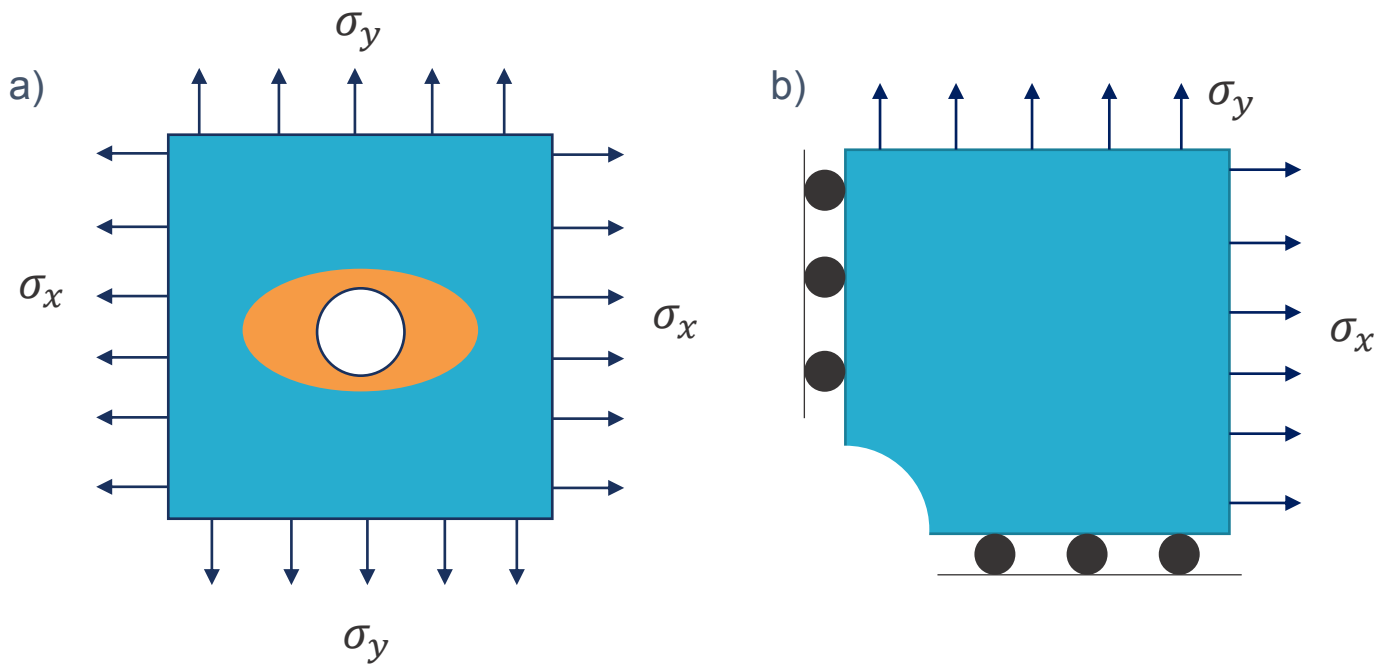

a) Schematic of the Galin Plate problem, a 2D benchmark problem with plane strain conditions. The plastic zone forms around the central hole. For the given loading, the plastic zone will be in the shape of an ellipse. b) Schematic of the model used in this analysis, with symmetry boundary conditions imposed.

Galin Plate – Comparison of Mesh Size

a)

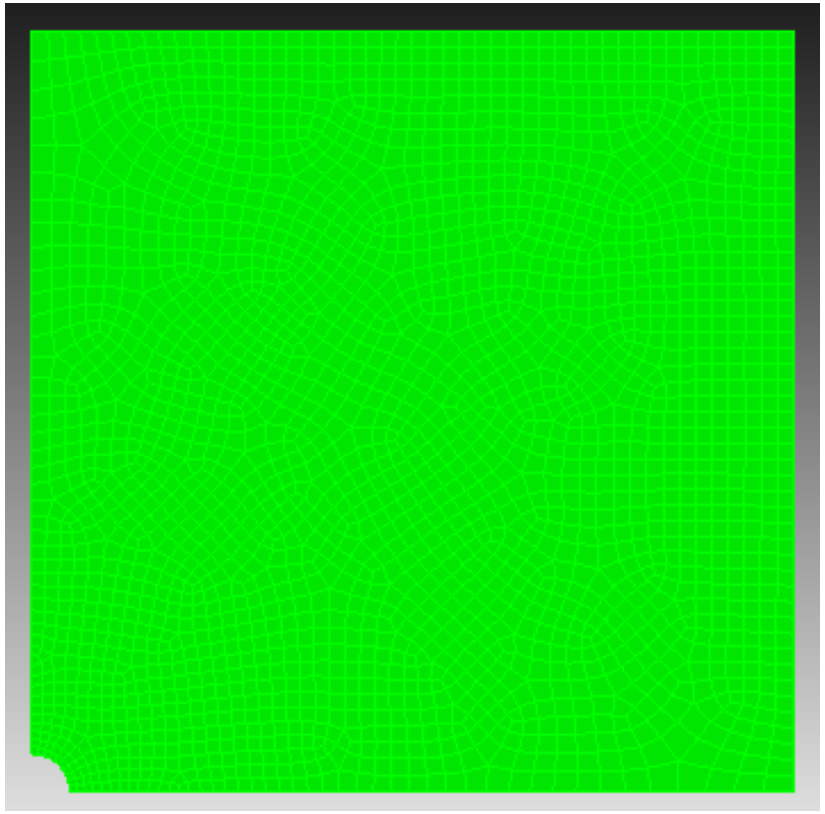

b)

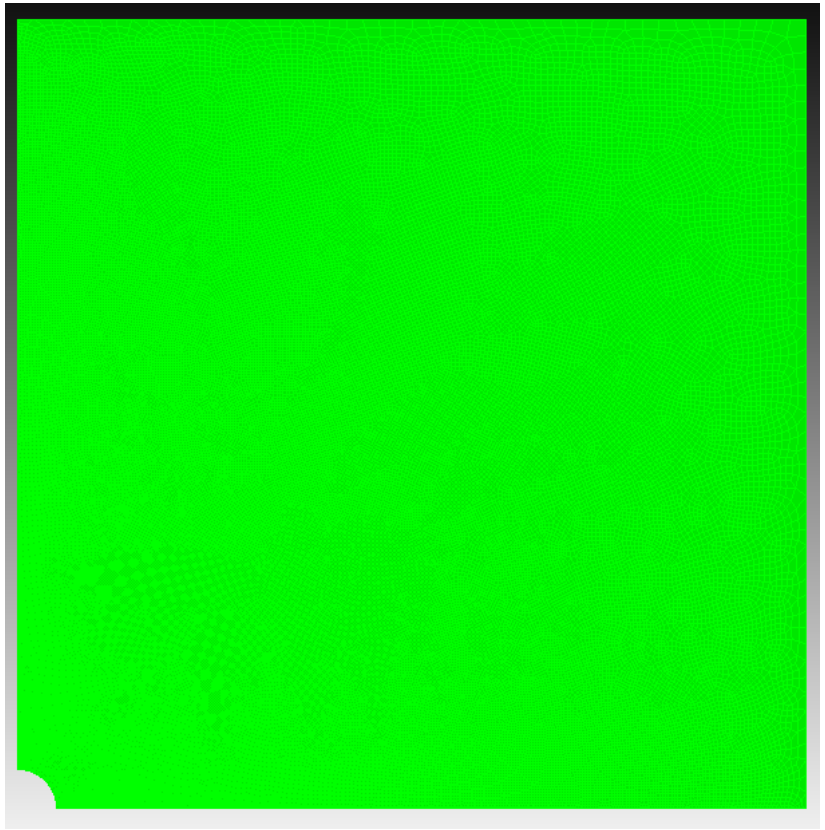

a) Galin plate quarter model coarse mesh, with 2377 elements b) Fine mesh, with 71,098 elements

- To investigate how the solution accuracy changes with respect to element size, two meshes are evaluated: a coarse mesh with 2377 elements and a fine mesh with 71, 098 elements

Galin Plate – Comparison of Mesh Size, Plastic Zone

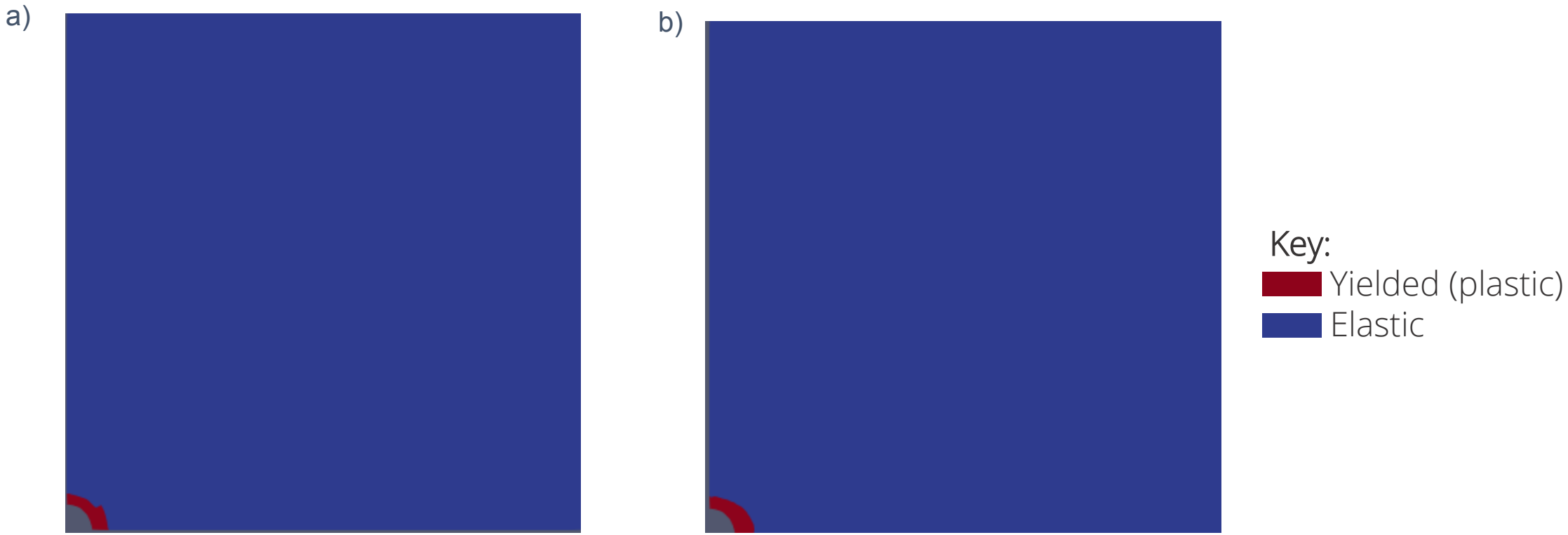

Visualization of plastic zone for a) Galin plate quarter model coarse mesh and b) Fine mesh

- For both mesh sizes, the shape of the plastic zone is elliptical, as expected from the analytical solution.
- The geometry of the elements of the coarse mesh limit the accuracy of the plastic zone size. The fine mesh's major and minor axes of the plastic zone match the analytical solution closely (within 10% error)

Galin Plate – Comparison of Mesh Size

a)

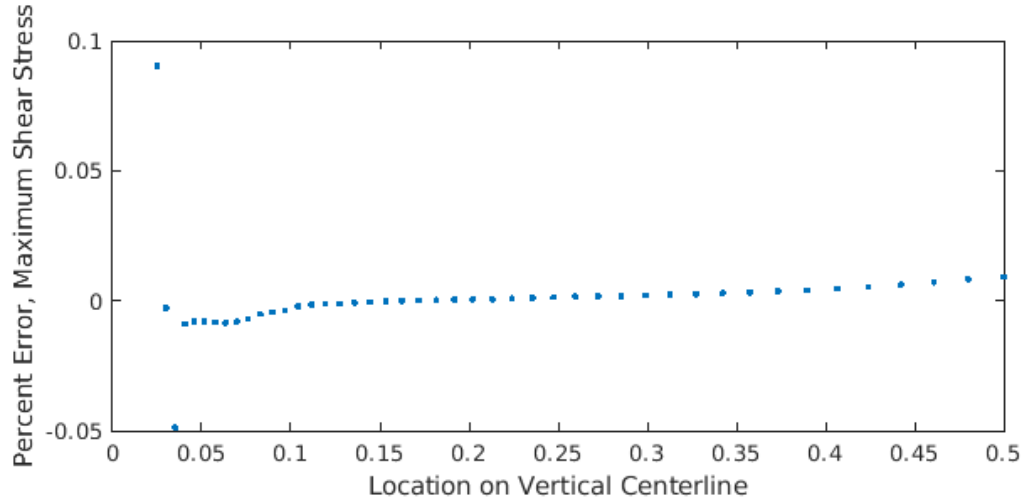

b)

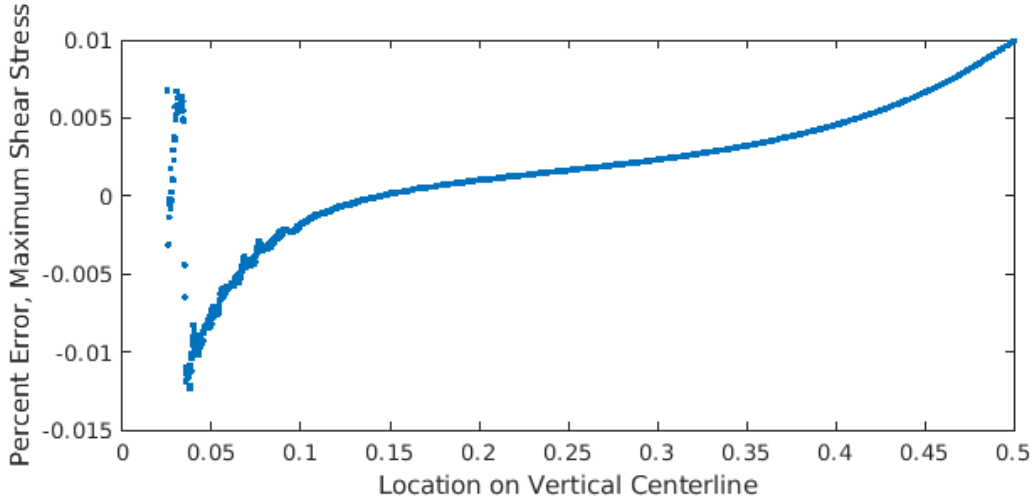

Percent error of the maximum shear stress in the mesh along the vertical red line of the Galin plate a) for coarse mesh and b) for fine mesh

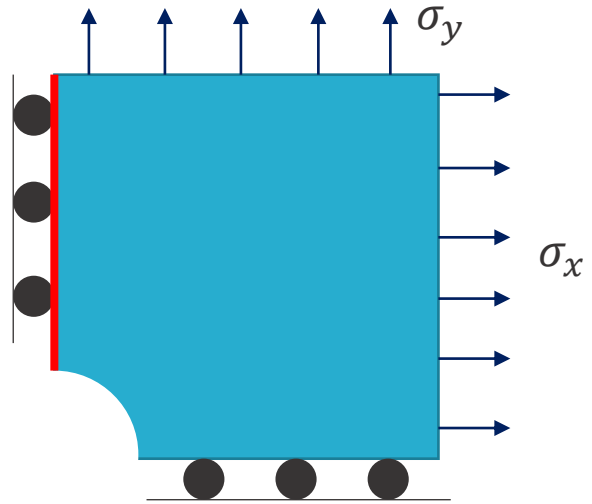

Schematic of Galin Plate quarter model, illustrating the location on vertical centerline that the maximum shear stress error is plotted against with a red line.

- Error is significantly reduced with a refined mesh
- Computational time (1.6s vs. 251s)
- Not possible to accurately match analytical solution where the infinite domain is assumed

Galin Plate – Comparison of Analytical and Sierra Solutions

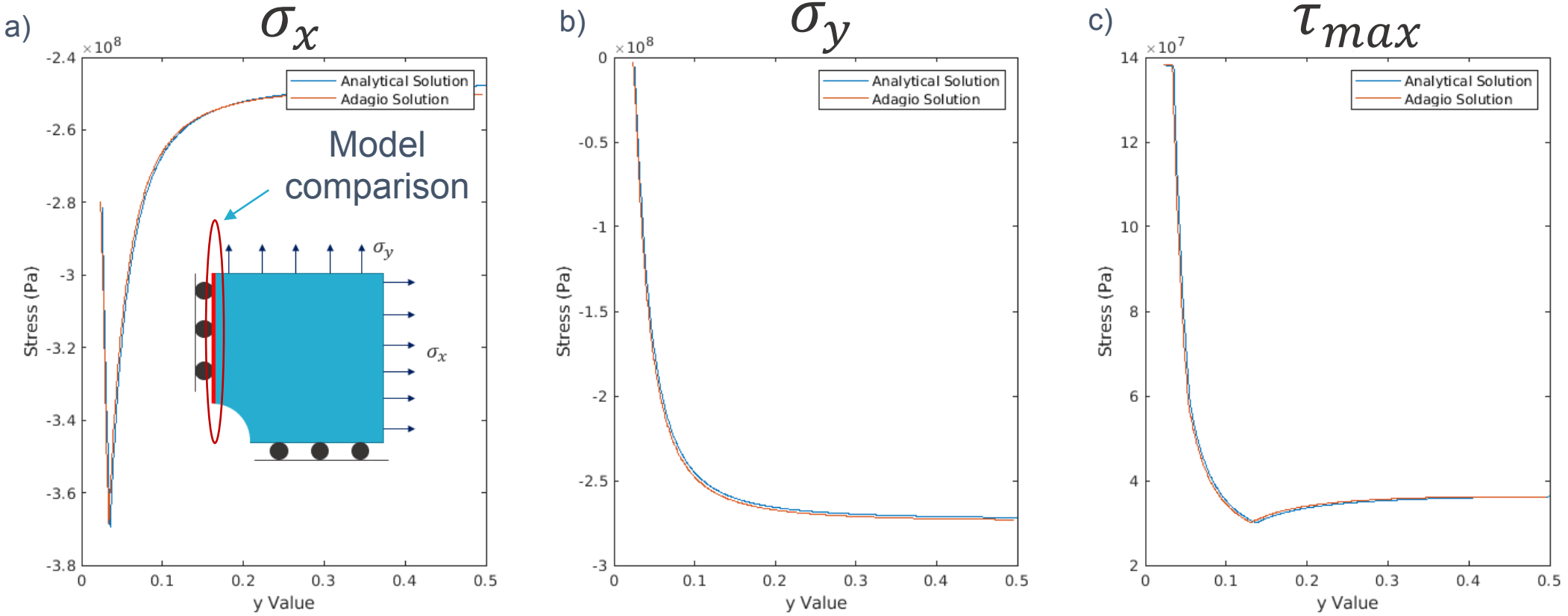

Comparison of Sierra Mechanics solution with Analytical solution along the vertical red line of the model, for a) Stress in the x-direction, b) Stress in the y-direction, and c) Maximum shear stress.

- The stresses predicted with Sierra S/M closely match the analytical solution

Error in Mean Stress, Entire Plate

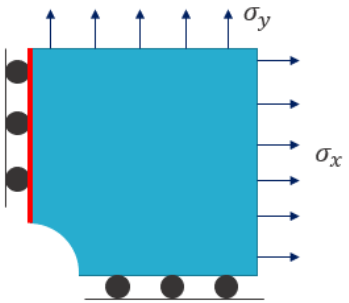

a)

b)

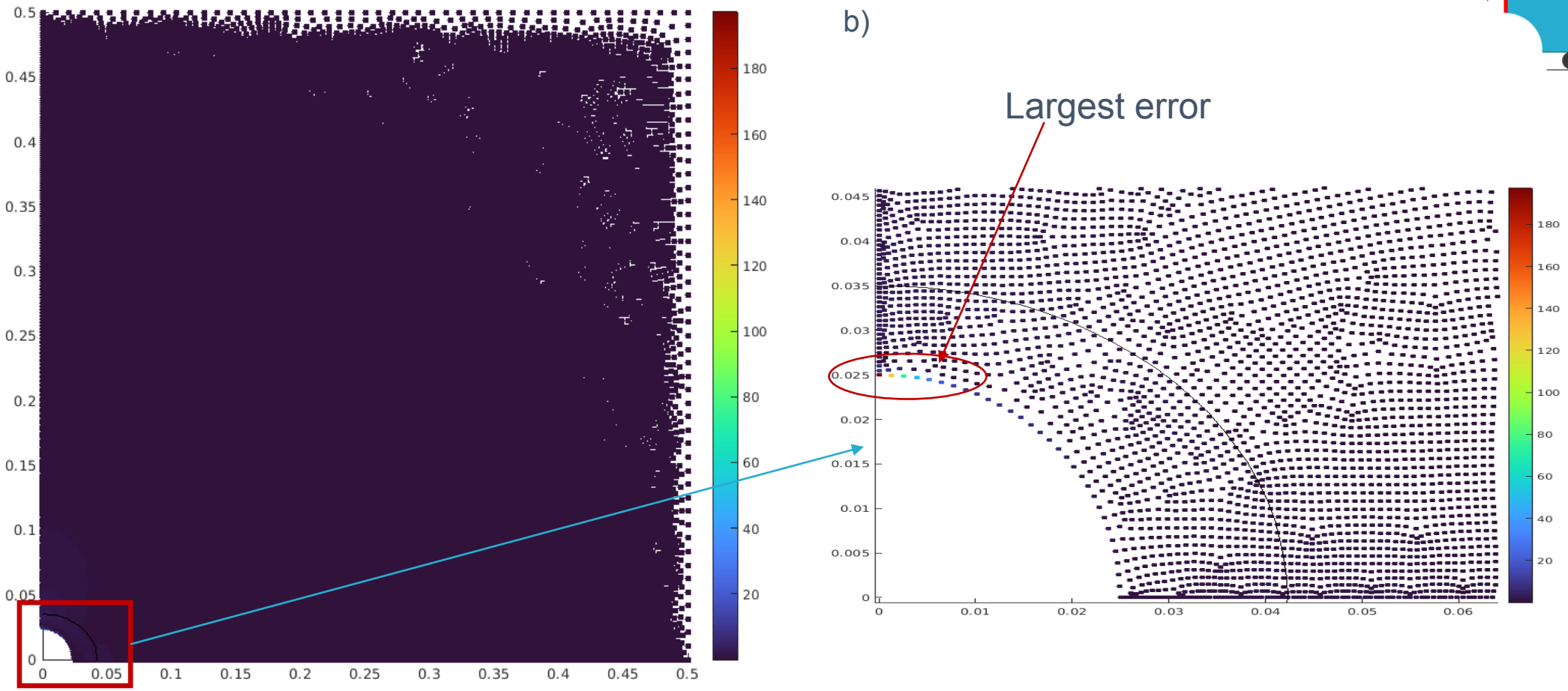

Plot of percent error at each node of the mesh, with x and y axes referring to the coordinates of the plate and the color of the points representing the magnitude of error. a) view of entire plate simulation and b) close view of the border near the hole. The plastic zone is outlines with a black line.

- The largest error in the Sierra simulation is at the boundary of the hole, and is large compared to the error within the rest of the plate

Conclusions and Future Work

- This work implemented plasticity into the fixed stress scheme for the Sandia Sierra Multiphysics toolkit
  - Use of Kayenta constitutive model
- Larger errors are expected at areas with high stress concentrations and at boundaries
  - Mesh refinement alleviates the degree of errors, but not completely
  - Due to the infinite assumption in analytical solution, model verification needs to be careful with boundary conditions
- Future Work
  - Utilize existing experimental data to calibrate Kayenta model and evaluate Sierra/Arpeggio results against experimental data for borehole breakout tests

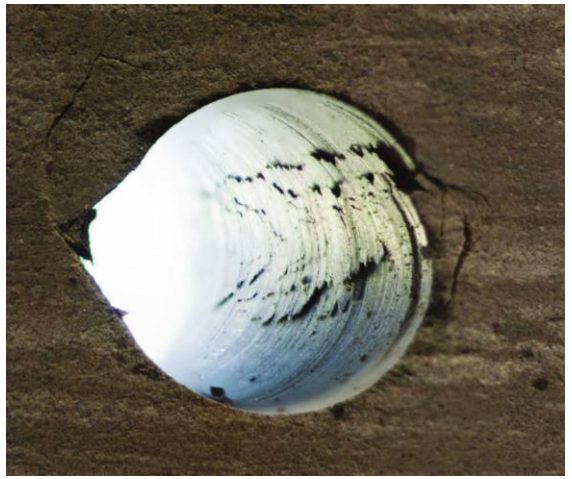

Choens et al., 2019 [10]

References

[1] Newell P, Martinez MJ. Numerical assessment of fault impact on caprock seals during CO2 sequestration. *Int J Greenh Gas Control*. Published online 2020. doi:10.1016/j.ijggc.2019.102890

[2] Kim J, Tchelepi HA, Juanes R. Stability, accuracy and efficiency of sequential methods for coupled flow and geomechanics. *SPE Reserv Simul Symp Proc*. 2009;2(January):802-821. doi:10.2118/119084-ms

[3] Brannon, Rebecca Moss, Fuller, Timothy Jesse, Strack, Otto Eric, Fossum, Arlo Frederick, and Sanchez, Jason James. KAYENTA: Theory and User's Guide. United States: N. p., 2015. Web. doi:10.2172/1238100

[4] Team STFD. *SIERRA Multimechanics Module: Aria User Manual - Version 5.0.*; 2021. doi:10.2172/1777075

[5] Beckwith, Frank and Bergel, Guy Leshem and de Frias, Gabriel Jose and Manktelow, Kevin and Merewether, Mark Thomas and Miller, Scott T and Mosby, Matthew David and Plews, Julia A. and Porter, Vicki L. and Shelton, Timothy and Thomas, Jesse David and Trewe EB. *Sierra/SolidMechanics 5.0 User's Guide*.; 2021. doi:10.2172/1608404

[6] Team STFD. *SIERRA Code Coupling Module: Arpeggio User Manual - Version 5.0.*; 2021. doi:10.2172/1777077

[7] Liu, M., & Huang, H. (2021). Finite element modeling of spherical indentation in a poro-elasto-plastic medium via step displacement loading. *International Journal for Numerical and Analytical Methods in Geomechanics*, *45*(10), 1347-1380.

[8] Dewers, T., Newell, P., Broome, S., Heath, J., & Bauer, S. (2014). Geomechanical behavior of cambrian mount simon sandstone reservoir lithofacies, iowa shelf, usa. *International Journal of Greenhouse Gas Control*, *21*, 33-48.

[9] Yarushina, V. M., Dabrowski, M., & Podladchikov, Y. Y. (2010). An analytical benchmark with combined pressure and shear loading for elastoplastic numerical models. *Geochemistry, Geophysics, Geosystems*, *11*(8).

[10] Choens, R. C., Lee, M. Y., Ingraham, M. D., Dewers, T. A., & Herrick, C. G. (2019). Experimental studies of anisotropy on borehole breakouts in Mancos Shale. Journal of Geophysical Research: Solid Earth, 124, 4119– 4141. https://doi.org/10.1029/2018JB017090.